



RESEARCH MEMORANDUM

EXPERIMENTAL INVESTIGATION OF THE EFFECTS OF SWEEPBACK
ON THE FLUTTER OF A UNIFORM CANTILEVER WING WITH
A VARIABLY LOCATED CONCENTRATED MASS

By Herbert C. Nelson and John E. Tomassoni

Langley Aeronautical Laboratory
Langley Air Force Base, Va.

CLASSIFICATION CANCELLED

CLASSIFIED DOCUMENT

Authority

J. W. Crowley Date *12/14/53*
EO 1.05016
1/11/54 See *note*
R71913

This document contains classified information affecting the National Defense of the United States within the meaning of the Espionage Act, USC 5031 and 5032. The transmission or the revelation of its contents in any manner to unauthorized persons is prohibited by law. Information so classified may be imparted only to persons in the military and naval services of the United States, and to civilian officers and employees of the Federal Government who have a legitimate interest therein, and to United States citizens of known loyalty and discretion who of necessity must be informed thereof.

NATIONAL ADVISORY COMMITTEE
FOR AERONAUTICS

WASHINGTON
August 31, 1949

UNCLASSIFIED



NATIONAL ADVISORY COMMITTEE FOR AERONAUTICS

RESEARCH MEMORANDUM

EXPERIMENTAL INVESTIGATION OF THE EFFECTS OF SWEEPBACK
ON THE FLUTTER OF A UNIFORM CANTILEVER WING WITH
A VARIABLY LOCATED CONCENTRATED MASS

By Herbert C. Nelson and John E. Tomassoni

SUMMARY

The results obtained from 95 subsonic flutter tests which were conducted in the Langley 4.5-foot flutter research tunnel on untapered cantilever wings with sweepback angles of 0° , 45° , and 60° and carrying a single concentrated weight are presented. The weight used throughout the series of tests was 14 percent heavier than each wing. A primary purpose of the investigation was to present experimental information to be used as a basis for evaluating analytical procedures for determining the flutter speed of weighted sweptback wings.

The weight was mounted at a series of spanwise positions on the leading edges and on the midchord lines of the wings. The results of the tests in which the wings were weighted at the leading edge indicated that the flutter speed was greatly affected by the spanwise position of the weight and, in these cases, the change in sweepback did not appreciably alter the flutter speed. For the cases in which the wings were weighted at the midchord, an increase in sweepback generally caused an increase in the flutter speed and, as the sweep angle was increased, the effect of the spanwise weight position became more pronounced. The results are presented in the form of plots of flutter speed and frequency as a function of spanwise weight position for the sweepback angles tested.

INTRODUCTION

The purpose of this paper is to present experimental data on the flutter characteristics of sweptback untapered cantilever wings carrying concentrated weights. These data were obtained from 95 flutter tests conducted in the Langley 4.5-foot flutter research tunnel on wings, each carrying a single weight at a series of spanwise

~~RESTRICTED~~

UNCLASSIFIED

positions on the leading edge and midchord line. The investigation covered sweepback angles of 0° , 45° , and 60° .

Several analytical methods have been devised for calculating the flutter speed of an unswept wing carrying an arbitrarily placed weight. The methods of reference 1, which treats a uniform unswept wing by a differential-equation method, and of reference 2, which treats a general unswept wing by using chosen modes, were appraised with the aid of the experimental data presented in reference 3. Reference 4, which presents a general analytical method for swept wings, does not explicitly develop the procedures for including a concentrated weight and comparison is made with experiment for uniform wings only. The present paper furnishes experimental data that can be used to examine methods for predicting the flutter speed of a weighted sweptback wing.

Because of the importance of the vibration characteristics in a flutter analysis, the nodal-line patterns associated with the second and third natural frequencies of the models at zero airspeed are presented. This information may serve to check the method used in a flutter analysis for analytically obtaining the coupled modes of vibration of a wing at zero airspeed.

The models were made from uniform thin sheet metal with their leading edges rounded off and, if destroyed by flutter, they could easily be reproduced. The models tested were practically the same in characteristics except as changed by sweepback.

Essentially one weight was used throughout the series of tests. This weight approximately simulated the mass characteristics of an engine. The results of tests as presented in this paper may be regarded qualitatively for the effects investigated and furthermore used quantitatively for comparison with subsequent analyses.

SYMBOLS

W	weight of wing model, pounds
W_w	weight of concentrated weight, pounds
l	length of midchord line, feet
b	half-chord of wing model measured perpendicular to midchord line, feet
t	thickness of wing section, inches

Λ	sweep angle, positive for sweepback, degrees
x_α	distance between elastic axis and center of gravity of wing section, referred to half-chord
e_w	distance between elastic axis of wing section and center of gravity of weight, referred to half-chord, negative for forward weight location
I_{CG}	mass moment of inertia of wing section about its center of gravity, inch-pound-second ² per inch
I_{EA}	mass moment of inertia of wing section about its elastic axis, inch-pound-second ² per inch
I_w	mass moment of inertia of weight about an axis parallel to leading edge through its center of gravity, inch-pound-second ²
EI	bending rigidity of wing section, pound-inch ²
GJ	torsional rigidity of wing section, pound-inch ²
m	mass of wing per unit length, slugs per foot
r_α	nondimensional radius of gyration of wing section about its elastic axis $\left(\sqrt{\frac{I_{EA}}{mb^2}} \right)$
q_f	dynamic pressure at flutter, pounds per square foot
ρ	air density, slugs per cubic foot
v_f	true-stream velocity at flutter, feet per second
κ	mass ratio $\left(\frac{\pi \rho b^2}{m} \right)$
ξ_h, ξ_α	structural damping coefficient in degree of freedom indicated by subscript
α	angle of attack of wing section, positive leading edge up
h	bending deflection of wing section at elastic axis, positive downward

APPARATUS

The Langley 4.5-foot flutter research tunnel was used for this series of tests. The testing medium was air under approximate atmospheric conditions.

The models used in the investigation were flat-plate cantilever wings made from 24S-T aluminum with their leading edges rounded off. The unswept model had a length of 3 feet, a chord of 0.667 foot, and a thickness of 0.0900 inch. Two sweptback models were used, one having a sweep angle of 45° and the other, 60° . The midchord lines of the swept models had a length of 3 feet, and the other properties were the same as for the unswept wing.

Each model was mounted as a vertical rigid cantilever wing with its root at the top of the test section parallel to the air stream. This type of mounting resulted in flutter involving no bending or torsional displacements of the root. The sweptback models were effectively obtained by rotating the unswept wing about the intersection of the midchord line and the root. A sketch of each model is shown, with its data in table I. The wing properties based on the unswept wing are as follows:

Chord, $2b$, feet	0.667
Length, l , feet	3
Aspect ratio (geometric)	4.5
Taper ratio	1
Airfoil section	Flat plate
g_h , nondimensional	0.01 (approx.)
g_α , nondimensional	0.005 (approx.)
Thickness, t , inches	0.0900
W , pounds	2.735
I_{CG} , inch-pound-second ² per inch	0.00995
I_{EA} , inch-pound-second ² per inch	0.00995
EI , pound-inch ²	0.00506×10^6
GJ , pound-inch ²	0.0080×10^6
x_α , nondimensional	0.0
r_α^2 , nondimensional	0.334
$1/k$ (standard air, no weight)	34.1
Λ , degrees	0

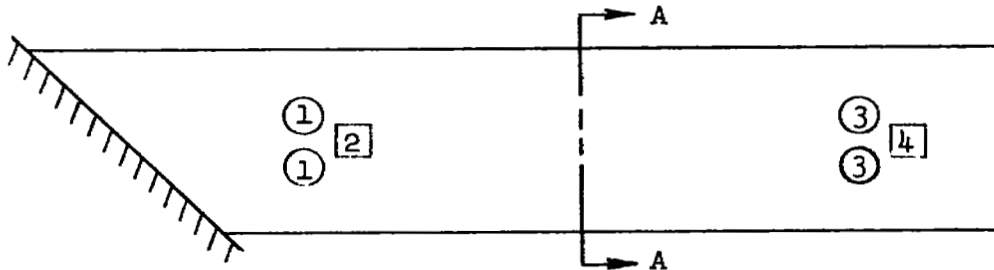
The elastic axis and center of gravity of the wing sections were located at midchord. Because of the type of mount used in the investigation, it was necessary to use three wing models, each having the same properties, except as changed by the sweepback angle.

Two weights which were essentially the same were used; one was moved along the leading edge and the other, along the midchord line of each model. The properties of the weights were as follows:

	Leading-edge weight	Midchord weight
W_w , pounds . .	3.12	3.12
e_w	-1.0	0
I_w	0.0100	0.0098

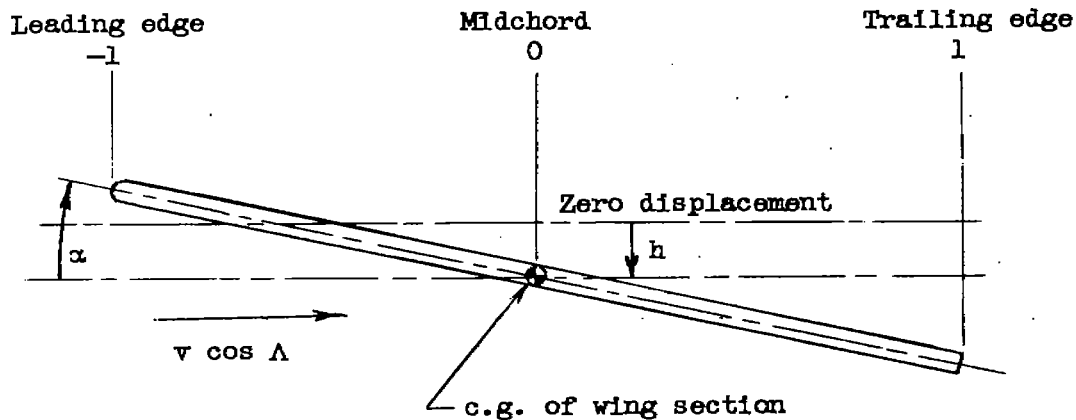
The two weights were each about 14 percent heavier than the wing.

Vibration records of the bending and torsional oscillations of the wing during flutter were obtained electrically by the use of strain gages cemented on the wing. The strain gages were connected through a system of bridges and amplifiers to a recording oscillograph. Two sets of gages were used on each model. One set of gages was mounted on the midchord line approximately 4 inches from the root and the other, on the same line about 4 inches from the tip. The approximate location of the strain gages is illustrated as follows:



The squares represent the bending gages and the circles, the torsion gages. The numbers 1, 2, 3, and 4 represent the root-torsion, root-bending, tip-torsion, and tip-bending gages, respectively.

The system used in obtaining the proper phase-angle relationship between the bending and torsional stresses of the wing as recorded in table I is as follows:

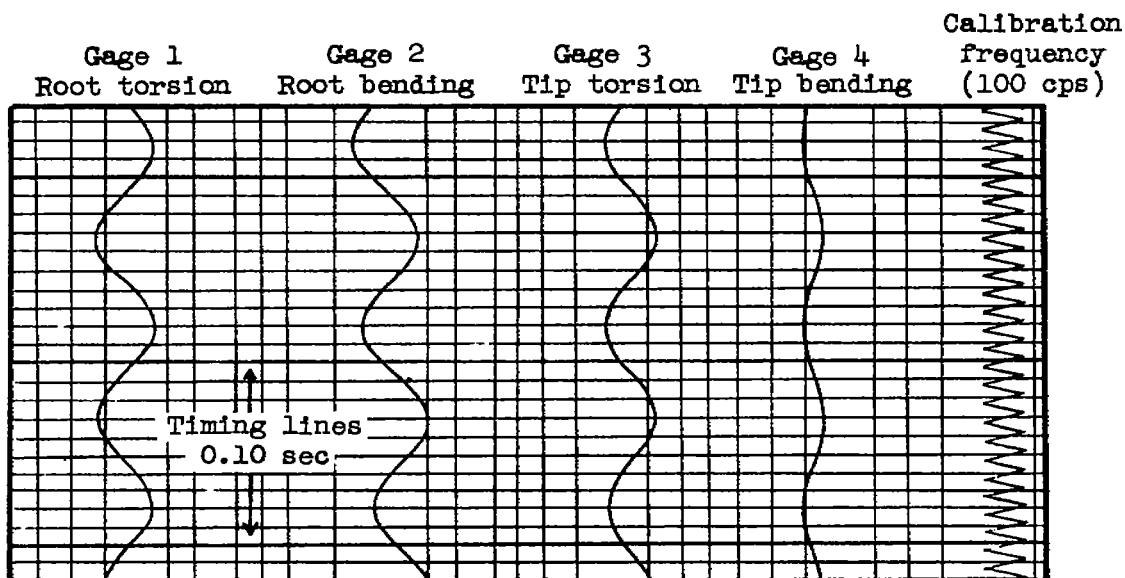


Section A-A

The preceding sketch shows the relative directions of positive bending (h) and torsional (α) displacements of the wing section. A couple, which twisted the wing in the positive α -direction, was applied at the tip. This action induced positive twist at each section of the wing; therefore, the direction in which the torsion-gage traces moved on the oscillograph record for positive twist at the gage stations was obtained. A force was then applied, which deflected the tip in the positive h -direction, thus producing positive bending curvature at each section of the wing; therefore, the direction in which the bending-gage traces moved on the oscillograph record for positive bending curvature at the gage stations was determined. Thus, the phase-angle relationships between the strain-gage traces on the oscillograph record for positive torsional and bending stress at the gage stations was established. Each model was treated in the same manner. The root-torsion-gage trace was used as a reference. If the traces of the other gages were displaced in the same direction as the reference-gage trace for positive twist or bending curvature, they were in phase (0°); if not, they were out of phase (180°). The following table gives the results of the calibration:

Model	Phase-angle relationship			
	Gage 1	Gage 2	Gage 3	Gage 4
A	Reference	180°	0°	180°
B	Reference	180°	0°	180°
C	Reference	0°	0°	0°

The way in which this table was used is illustrated with the aid of the following sample oscillograph record:



If the record is assumed to be obtained from any one of the models, the phase-angle relationship between the bending and torsional stresses of the model at the strain gages would be obtained as follows:

Model	Gage 1	Gage 2	Gage 3	Gage 4
A	Reference	0°	180°	0°
C	Reference	180°	180°	180°

The gage traces on the sample oscillograph record are numbered and labeled and for all the records of figure 1 and data of table I the identification is the same.

TEST PROCEDURE

Since flutter is usually destructive, recognition of flutter, recording of the necessary data, and reduction of the airspeed to save the model must be accomplished in a very short time. The airspeed was increased slowly, and at the flutter point, oscillograph records were taken and the tunnel conditions were recorded. The first three natural frequencies of each model at zero airspeed for the various weight positions were recorded before the model was flutter-tested. After each model had been made to flutter with various weighted conditions, it was retested with no weight to establish whether or not it had been damaged by flutter. In addition, the nodal-line patterns associated with the second and third natural frequencies of the models at zero airspeed (fig. 2) were obtained.

PRESENTATION OF RESULTS

Experimental results, obtained from the flutter tests of wings with sweepback angles of 0° , 45° , and 60° and carrying a single concentrated weight at a series of spanwise and two chordwise positions, are presented in table I and in figures 3 and 4. In table I the quantities listed are dynamic pressure, flutter velocity, Mach number, natural and flutter frequencies, and phase-angle relationships of the bending and torsional stresses for the corresponding second and third natural and flutter frequencies. A sketch of each model configuration is included in the table with its corresponding data.

The oscillograph records taken at flutter for the 95 flutter tests are shown in figure 1. The gage traces in the records are numbered from left to right and are: (1) root torsion, (2) root bending, (3) tip torsion, and (4) tip bending. The gage traces are marked at the top of each record with their appropriate attenuations. The run numbers are given in the lower left-hand corner of each record.

The second and third natural-frequency nodal lines of each model configuration-weighted at the leading edge are shown in figure 2. The progressive change in these nodal lines with spanwise weight position is illustrated.

In figure 3 the first three natural frequencies and the flutter frequency are plotted against spanwise weight position for each sweep angle and chordwise weight position. These plots show the relation between the flutter frequency and the first three natural frequencies of the wing for a given weight position.

The variation of the flutter velocity with spanwise weight position for the configurations weighted at the leading edge and those weighted at the midchord are shown in figures 4(a) and 4(b), respectively.

DISCUSSION OF RESULTS

The models used in the series of tests were solid metal cantilever wings with thin rectangular cross sections and could easily be reproduced in case flutter proved to be destructive. These models were of such a nature that they fluttered at low Mach numbers. The lifting characteristics of the airfoil section used are approximately the same as those of a conventional airfoil with the exception that flow separation associated with the stalling condition occurs at a lower angle of attack. Since the model was mounted at essentially a zero angle of attack, it is very unlikely that the flutter speed was appreciably influenced by this separation effect.

The first three natural frequencies, the flutter frequency, and the flutter velocity of each model configuration tested are given in table I. The quantities have been plotted in figures 3 and 4. The figures show that, in general, a marked change in flutter frequency and a large increase in the flutter speed occurred when the weight was located between 40 and 80 percent of the wing length.

The variation in flutter velocity due to a variation of sweepback for a given chordwise and spanwise position of the weight is shown in figure 4. The second and third natural modes of vibration of the models weighted at the leading edge (fig. 4(a)) were of a highly coupled nature as shown by figure 2. Apparently this large amount of coupling had a greater effect on the flutter speed than did sweepback. In general, for this leading-edge weight position, variation in sweepback did not cause a large difference in flutter speed. The major effect on the flutter speed of the models weighted at the leading edge was due to the spanwise location of the weight.

In figure 4(b) the flutter velocities of the models weighted at the midchord are presented. In this case the mass coupling was relatively small. As is noted in figure 4(b), the effect of sweepback was more pronounced. The flutter velocity of the unswept wing was not greatly affected by spanwise weight position. When the wing was swept back, however, spanwise weight position did have an effect, probably because sweepback induced an amount of coupling which was further increased by the addition of the weight to the wing.

An unswept wing carrying a single weight on the leading edge was experimentally investigated in reference 3 and analytically investigated

in reference 1. The ratios of the weights and mass moment of inertias ($\frac{W_w}{W}$ and $\frac{I_w}{I}$) used in the reference papers were approximately the same as those used in this paper. In reference 3 and this paper a complete spanwise survey of the unswept wing could not be experimentally obtained because the flutter velocity exceeded the divergence velocity over a large range of weight positions. However, a complete spanwise survey of the wing in reference 3 was analytically obtained in reference 1. It is of interest to mention that the trend with spanwise position of the analytical results obtained in reference 1 for an unswept wing was similar to that reported in this paper for the swept wings, each being weighted at the leading edge.

Two flutter speeds were obtained from the unswept, unweighted wing. In the neighborhood of the lower flutter speed the flutter was not of a destructive nature and the lower speed range could be exceeded and the higher flutter speed obtained. The flutter occurring at the lower speed appeared to involve a significant amount of wing second bending, and at the higher speed the model appeared to vibrate very little in bending and its motion was predominantly torsional. The unweighted, unswept wing was the only model for which two flutter velocities were recorded. All other flutter velocities reported herein were the lowest values obtained regardless of the violence of the flutter.

In table I several of the recorded flutter frequencies are marked. The flutter in these cases was of an unusual nature. (See fig. 1.) Consider run 71, for example, in which case two distinct frequencies were obtained simultaneously at flutter. This case was unexpected since flutter usually involves only one frequency or, in some cases, occurs with a burst of one frequency, then a burst of a different frequency. Run 71 (weight at 41.67 percent l) was not an isolated case unrelated to those in which the weight position was nearby on either side. As the weight was moved spanwise (runs 67 to 74) the model experienced a change in flutter mode. The amplitude of the tip gage traces diminished as the weight was moved toward the tip of the wing (runs 67 to 70). In run 71 the tip traces came in at a higher frequency, and a high frequency persisted on the tip traces in runs 71 to 74. The root traces, on the other hand, had a relatively constant amplitude and frequency in runs 67 to 71 and then were inactive in runs 72 to 74. On the basis of the records presented in figure 1, run 71 can be considered to be part of a flutter-mode change.

A possible explanation of such an unusual type of flutter is that the flexibility of the thin plate-like structure and the associated nodal-line patterns may be involved. Furthermore, these models had low structural damping.

Table I contains the phase-angle relationships between the torsional and bending stresses of the second and third natural frequencies and the flutter modes of vibration of each of the models tested. The phase angles pertaining to the flutter modes were read from records, portions of which are shown in figure 1. The phase angles pertaining to the natural modes were read from records not appearing in this paper. All the phase angles were obtained using the system illustrated in the section on apparatus. It should be kept in mind that these phase angles relate the wing stresses at the gage stations and not the deflections. In order to obtain a deflection curve, the spanwise stress or moment distribution must be known. Since the wings tested carried only two sets of gages, this spanwise distribution was not obtained. Thus, if the tip and root bending stresses are out of phase, it merely indicates that there is at least one inflection point in the mode shape but not necessarily a nodal point. On the records in figure 1, the various gage traces are marked with their appropriate attenuations. Since the amplitude of the gage trace is inversely proportional to its attenuation for a given stress and the amplitude is directly proportional to the stress, the bending moment at the root may be approximately related to the bending moment at the tip and the torque at the root to the torque at the tip. The relative bending moments and torques and the phase angles between bending and torsion at two stations on the wing can give no direct information as to the flutter mode but might be used as a check on results obtained analytically.

The large amount of coupling present when the weight was located on the leading edge of the wings is clearly illustrated by the sketches shown in figure 2. Note that the third natural frequency was of a torsional nature when the weight was near the root but changed to one of a second-bending nature as the weight neared the tip of the wing, and, conversely for the second natural frequency. Figure 2 also serves to illustrate that sweepback alone induced coupling.

The sketches of the models indicate that the roots were parallel to the air stream. An investigation of the effect of a change in root restraint on the models tested would be desirable.

CONCLUDING REMARKS

The effect of sweepback on the flutter characteristics of a uniform cantilever wing carrying a concentrated weight has been experimentally investigated. The results as presented may be used in conjunction with analytical methods of predicting the flutter speed of sweptback wings carrying concentrated weights to indicate the validity of the methods used.

Wings carrying a single weight (14 percent heavier than the wing) at a series of spanwise positions on the leading edge and on the midchord line were tested at sweepback angles of 0° , 45° , and 60° . A comparison of the results obtained from the tests in which the wings were weighted at the leading edge indicated that the flutter speed was greatly affected by variation of spanwise weight position, and in these cases the change in sweepback angle had a small effect on the flutter speed. For the wings weighted at the midchord, the general effect of increase in sweepback was to increase the flutter speed and, as the sweep angle was increased, the effect of spanwise weight position became more pronounced.

Langley Aeronautical Laboratory
National Advisory Committee for Aeronautics
Langley Air Force Base, Va.

REFERENCES

1. Runyan, Harry L., and Watkins, Charles E: Flutter of a Uniform Wing with an Arbitrarily Placed Mass According to a Differential-Equation Analysis and a Comparison with Experiment. NACA TN 1848, 1949.
2. Woolston, Donald S., and Runyan, Harry L.: Appraisal of Method of Flutter Analysis Based on Chosen Modes by Comparison with Experiment for Cases of Large Mass Coupling. NACA TN 1902, 1949.
3. Runyan, Harry L., and Sewall, John L.: Experimental Investigation of the Effects of Concentrated Weights on Flutter Characteristics of a Straight Cantilever Wing. NACA TN 1594, 1948.
4. Barmby, J. G., Cunningham, H. J., and Garrick, I. E.: Investigation of the Effects of Sweep on the Flutter of Cantilever Wings. NACA RM L8H30, 1948.

TABLE I.- EXPERIMENTAL DATA

Model	Run	q_f (lb/sq ft)	V_f (fps)	Mesh number	Distance of weight from root (percent l)	Frequencies (cps)				Phase-angle relationship of bending and torsional stresses. (Ref indicates reference strain-gage traces)											
						Natural			Flutter	2nd natural mode				3rd natural mode				Flutter mode			
						1st	2nd	3rd		1	2	3	4	1	2	3	4	1	2	3	4
Model A Unswept untapered wing Weight moved along leading edge; $c_w = -1$ Reynolds number $\frac{\rho V_f l}{\mu} = 3693.1 V_f$	1	33.29	175.8	0.1515	0	2.24	13.65	19.64	21.00 *12.00	---	Ref	-	180	Ref	---	0	---	---	--	--	---
	2	16.05	121.5	.1045	0	2.24	13.65	19.64	14.75	---	Ref	-	180	Ref	---	0	---	Ref	36	0	216
	3	16.99	125.1	.1075	5.55	2.26	13.64	19.38	14.80	---	Ref	-	180	Ref	---	0	---	Ref	35	0	217
	4	28.21	161.5	.1389	11.11	2.26	12.88	17.48	10.04	Ref	180	-	0	Ref	0	0	180	Ref	0	0	0
	5	27.86	160.5	.1379	16.66	2.25	10.78	16.24	8.51	Ref	---	-	---	Ref	0	0	180	Ref	32	0	32
	6	28.30	161.9	.1390	22.20	2.23	8.83	16.15	7.41	Ref	---	-	0	Ref	0	0	180	Ref	50	22	356
	7	33.91	177.6	.1525	27.77	2.20	7.82	16.25	6.51	Ref	180	-	0	Ref	0	0	180	Ref	36	35	3
	8	35.18	172.3	.1480	33.33	2.14	7.11	16.25	Divergence	Ref	0	-	0	Ref	0	0	180	---	--	--	---
	---	---	---	---	38.90	2.07	6.85	15.98	Divergence	Ref	180	-	0	Ref	0	0	180	---	--	--	---
	---	---	---	---	44.40	1.97	6.82	15.75	Divergence	Ref	180	-	0	Ref	0	0	180	---	--	--	---
	---	---	---	---	50.00	1.85	7.11	15.46	Divergence	Ref	180	-	0	Ref	0	0	180	---	--	--	---
	---	---	---	---	55.50	1.74	7.52	15.01	Divergence	Ref	180	-	0	Ref	0	0	180	---	--	--	---
	---	---	---	---	61.11	1.63	8.18	14.62	Divergence	Ref	180	0	0	Ref	0	0	180	---	--	--	---
---	---	---	---	66.66	1.53	8.82	14.22	Divergence	Ref	---	0	0	Ref	0	0	180	---	--	--	---	
---	---	---	---	72.20	1.44	9.61	13.80	Divergence	Ref	0	0	0	Ref	0	0	180	---	--	--	---	
9	35.49	181.9	.1560	80.50	1.38	10.08	13.62	Divergence	Ref	0	0	0	Ref	0	-	180	---	--	--	---	
10	22.94	145.8	.1250	83.30	1.27	10.12	13.68	11.80	Ref	0	0	0	Ref	180	0	0	Ref	99	0	319	
11	12.34	106.9	.0915	88.90	1.18	9.77	13.85	*12.09	Ref	0	0	180	Ref	180	0	0	Ref	43	0	---	
12	10.62	98.6	.0845	94.40	1.12	9.21	14.01	12.09	Ref	0	0	180	Ref	180	0	0	Ref	123	0	230	
13	10.28	97.4	.0835	98.60	1.06	8.69	14.03	12.12	Ref	0	0	180	Ref	180	0	0	Ref	77	0	337	

*Note oscillograph record, figure 1.

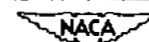


TABLE I.- EXPERIMENTAL DATA - Continued

Model	Run	U_p (lb/sq ft)	V_p (fps)	Mesh number	Distance of weight from root (percent l)	Frequencies (cps)				Phase-angle relationship of bending and torsional stresses. (Ref indicates reference strain-gage trace)											
						Natural			Flutter	2nd natural mode		3rd natural mode		Flutter mode							
						1st	2nd	3rd		1	2	3	4	1	2	3	4				
Model A Unswept untapered wing Weight moved along midchord line; $\alpha_p = 0$ Reynolds number $\approx 3775.7V_p$	14	17.23	129.1	0.1120	0	2.22	13.47	19.33	14.37	-	Ref	-	180	Ref	-	0	-	Ref	18	0	198
	15	19.00	131.7	.1135	5.75	2.30	13.33	19.48	14.63	-	Ref	-	180	Ref	-	0	-	Ref	26	0	226
	16	28.38	161.2	.1390	22.20	2.27	10.00	19.40	12.38 24.75	-	Ref	-	180	Ref	-	0	-	---	---	-	---
	17	28.40	161.3	.1390	27.77	2.24	8.95	18.92	10.81	-	Ref	-	180	Ref	-	0	-	Ref	0	0	4
	18	29.65	164.9	.1420	33.33	2.19	8.29	18.37	10.85	-	Ref	-	180	Ref	-	0	-	Ref	0	0	8
	19	29.02	163.1	.1405	38.90	2.06	8.03	17.80	10.60	-	Ref	-	180	Ref	-	0	-	Ref	0	0	25
	20	27.40	158.5	.1365	44.40	2.02	8.05	17.22	11.85	-	Ref	-	180	Ref	-	0	-	Ref	0	0	0
	21	31.84	171.2	.1475	50.00	1.89	8.43	16.69	8.00	-	Ref	-	180	Ref	-	0	-	Ref	0	0	180
	22	32.33	172.5	.1485	55.90	1.78	9.09	16.29	8.20	-	Ref	-	180	Ref	-	0	-	Ref	346	-	130
	23	31.73	170.3	.1466	61.11	1.67	10.07	15.99	8.63	-	Ref	-	180	Ref	-	0	-	Ref	0	0	0
	24	32.45	169.0	.1490	66.66	1.59	11.38	15.60	7.74	-	Ref	-	180	Ref	-	0	-	Ref	34	-	217
	25	33.77	172.5	.1520	72.20	1.49	12.76	15.36	7.23 28.90	-	Ref	-	180	Ref	-	0	-	---	---	-	---
	26	33.76	172.7	.1520	77.80	1.39	13.04	15.00	6.25 18.50	-	Ref	-	180	Ref	-	0	-	---	---	-	---
	27	9.00	28.9	.0780	83.30	1.30	12.96	14.81	13.14	-	Ref	-	180	Ref	-	0	-	Ref	73	0	240
28	10.06	34.2	.0825	94.40	---	---	---	12.70	-	---	-	---	---	-	-	-	Ref	34	0	221	

*Note oscillograph record, figure 1.



TABLE I.- EXPERIMENTAL DATA -- Continued

Model	Run	q_f (lb/sq ft)	v_f (fps)	Mach number	Distance of weight from root (percent l)	Frequencies (cps)				Phase-angle relationship of bending and torsional stresses. (Ref indicates reference strain-gage trace)											
						Natural			Flutter	2nd natural mode				3rd natural mode				Flutter mode			
						1st	2nd	3rd		1	2	3	4	1	2	3	4	1	2	3	4
Model B Swept untapered wing; $\Lambda = 45^\circ$ Weight moved along leading edge; $a_w = -1$ Reynolds number $\frac{\rho v_f l}{\mu} = 5310.2v_f$	29	29.42	162.0	0.1419	-11.11	2.47	14.91	20.30	11.12	Ref	-	-	0	Ref	0	0	180	Ref	24	0	24
	30	29.29	161.8	.1416	0	2.48	14.91	20.23	11.28	Ref	-	-	0	Ref	0	0	180	Ref	0	0	0
	31	27.22	156.2	.1365	5.55	2.48	14.54	18.87	11.38	Ref	0	-	0	Ref	0	0	180	Ref	0	0	0
	32	25.30	150.6	.1315	11.11	2.48	12.81	17.20	10.24	Ref	0	-	0	Ref	0	0	180	Ref	11	0	11
	33	22.13	140.9	.1229	16.66	2.46	10.51	17.24	8.96	Ref	0	-	0	Ref	0	0	180	Ref	0	0	0
	34	20.51	135.7	.1183	22.20	2.44	8.82	17.59	7.85	Ref	0	-	0	Ref	0	0	180	Ref	0	0	0
	35	21.10	137.7	.1200	27.77	2.41	7.75	17.89	6.79	Ref	0	-	0	Ref	0	0	180	Ref	0	0	0
	36	27.84	158.4	.1380	33.33	2.38	7.09	18.02	6.25	Ref	0	-	0	Ref	0	0	180	Ref	24	0	24
	37	53.17	219.8	.1918	38.90	2.27	6.76	18.00	5.96	Ref	0	-	0	Ref	0	0	180	Ref	162	0	162
	38	99.90	296.5	.2585	44.40	2.16	6.75	17.83	*16.35	Ref	0	-	0	Ref	0	0	180	Ref	0	0	---
	39	114.50	327.9	.2855	50.00	2.04	6.96	17.54	*16.96	Ref	0	-	0	Ref	0	0	180	Ref	0	0	---
	40	143.50	364.8	.3213	55.90	1.91	7.35	17.21	*18.47	Ref	0	-	0	Ref	0	0	180	Ref	12	12	0
	41	155.80	382.7	.3357	61.11	1.78	7.94	16.88	*28.6	Ref	0	-	0	Ref	0	0	180	Poor record			
	42	159.60	389.1	.3400	66.66	1.65	8.73	16.42	27.60 *5.52	Ref	0	-	0	Ref	0	0	180	Ref	0	0	180
	43	161.20	392.7	.3421	72.20	1.54	9.52	15.84	21.20 *5.30	Ref	0	0	0	Ref	0	0	180	Ref	0	--	180
	44	75.18	264.2	.2290	77.80	1.41	10.30	15.26	15.88	Ref	0	0	0	Ref	0	0	180	Ref	0	0	0
	45	33.89	176.4	.1525	83.30	1.33	10.74	14.78	13.70	Ref	0	0	0	No record				Ref	0	0	0
	46	14.16	113.5	.0980	88.90	1.24	10.91	14.11	13.13 *39.0	Ref	0	0	---	Ref	-	-	0	---	---	--	---
47	9.55	93.3	.0805	94.40	1.16	10.48	13.90	12.45 *17.40	Ref	0	0	180	Ref	0	0	0	---	---	--	---	
48	8.52	88.1	.0760	98.60	1.10	9.92	13.63	12.50	Ref	0	0	180	Ref	0	0	0	Ref	4	0	328	

*Note oscillograph record, figure 1.

TABLE I.- EXPERIMENTAL DATA - Continued

Model	Run	q_r (lb/sq ft)	V_r (fps)	Mach number	Distance of weight from root (percent l)	Frequencies (cps)				Phase-angle relationship of bending and torsional stresses. (Ref indicates reference strain-gage trace)											
						Natural			Flutter	2nd natural mode			3rd natural mode			Flutter mode					
						1st	2nd	3rd		1	2	3	4	1	2	3	4				
Model B Swept untapered wing; $\Lambda = 45^\circ$ Weight moved along midchord line; $\alpha_w = 0$ Reynolds number $\approx 5117.5V_r$	49	27.02	157.4	0.1355	0	2.50	14.89	20.18	11.11	Ref	---	-	0	Ref	0	0	180	Ref	24	0	24
	50	26.75	156.9	.1350	11.11	2.49	14.58	20.25	11.01	Ref	0	-	0	Ref	0	0	180	Ref	0	0	15
	51	27.00	157.7	.1355	16.66	2.48	14.08	20.00	10.80	Ref	0	-	0	Ref	0	0	180	Ref	0	0	0
	52	26.66	156.6	.1345	27.77	2.47	10.51	20.00	9.24	Ref	0	-	0	Ref	0	0	180	Ref	350	0	343
	53	28.33	161.7	.1389	33.33	2.40	9.45	18.87	8.60	Ref	0	-	0	Ref	0	0	---	Ref	0	0	0
	54	35.99	182.6	.1569	38.90	2.31	8.97	18.57	8.33	Ref	0	-	0	Ref	0	0	---	Ref	0	0	0
	55	41.03	195.1	.1675	44.40	2.20	8.87	18.00	14.71	Ref	0	-	0	Ref	0	0	---	Ref	0	0	0
	56	41.03	195.1	.1675	50.00	2.06	9.33	17.19	13.56	Ref	0	-	0	Ref	0	0	---	Ref	0	0	0
	57	37.68	187.1	.1605	55.50	1.93	9.78	16.81	^a 13.13	Ref	---	-	0	Ref	0	0	---	Ref	0	0	---
	58	48.25	212.2	.1820	61.11	1.80	10.86	16.39	^a 9.89	Ref	---	-	0	Ref	0	0	180	Ref	0	0	---
	59	43.70	201.9	.1730	66.66	1.67	12.31	16.22	7.72	Ref	---	-	0	Ref	0	0	180	Ref	0	0	---
	60	40.80	194.9	.1670	72.20	1.55	13.50	16.11	7.50	Ref	---	-	0	Ref	0	0	180	Ref	0	0	---
	61	37.71	187.5	.1605	77.80	1.45	14.06	16.33	6.99	Ref	0	0	0	Ref	0	0	180	Ref	0	0	---
	62	35.82	182.8	.1565	83.30	1.35	13.75	16.13	^a 5.71	Ref	0	0	0	Ref	0	0	180	Ref	0	0	---
	63	31.00	170.0	.1455	94.40	1.16	11.90	15.28	4.35	Ref	180	0	0	Ref	0	0	180	Ref	0	0	0

^aNote oscillograph record, figure 1.



TABLE I.- EXPERIMENTAL DATA - Continued

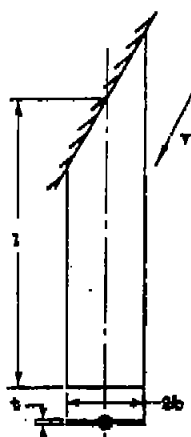
Model	Rin	q_r (lb/sq ft)	V_r (fps)	Mach number	Distance of weight from root (percent l)	Frequencies (ops)				Phase-angle relationship of bending and torsional stresses. (Ref indicates reference strain-gage trace)												
						Natural			Flutter	2nd natural mode				3rd natural mode				Flutter mode				
						1st	2nd	3rd		1	2	3	4	1	2	3	4	1	2	3	4	
		(deg)		(deg)		(deg)				(deg)		(deg)		(deg)		(deg)						
Model G Swept untapered wing; $\Lambda = 60^\circ$ Weight moved along leading edge; $a_y = -1$ Reynolds number $\approx 7306.2V_r$	64	40.92	192.7	0.1670	-19.44	2.94	17.52	22.35	13.33	Ref	180	-	0	Ref	0	0	180	Ref	180	14	24	
	65	40.72	193.1	.1670	0	2.93	17.55	21.54	13.62	Ref	180	-	0	Ref	0	0	180	Ref	180	14	19	
	66	33.50	174.6	.1510	13.88	2.92	13.70	19.7	11.41	Ref	0	0	0	Ref	0	0	---	Ref	---	0	0	
	67	30.98	158.2	.1450	19.44	2.92	11.43	-----	10.19	Ref	0	0	0	No record				Ref	36	14	18	
	68	25.94	153.8	.1325	25.00	2.88	9.71	20.51	8.75	Ref	---	-	0	---	Ref	-	180	Ref	55	12	30	
	69	27.78	159.2	.1373	30.55	2.88	8.40	20.83	8.12	Ref	180	-	0	Ref	0	0	180	Ref	64	33	39	
	70	36.84	183.3	.1585	36.11	2.80	7.74	21.21	7.01	Ref	180	0	0	Ref	0	0	180	Ref	105	105	79	
	71	96.88	299.3	.2600	41.67	2.70	7.32	20.83	^{6.79} _{30.40}	Ref	180	0	0	Ref	0	0	180	Refer to record				
	72	126.10	343.3	.2989	47.22	2.53	7.35	20.51	² 34.20	Ref	180	0	0	Ref	0	0	180	Refer to record				
	73	142.70	366.1	.3189	52.77	2.38	7.59	20.33	² 37.90	Ref	180	0	0	Ref	0	0	180	Refer to record				
	74	222.00	465.8	.4050	58.33	2.13	8.10	20.00	^{6.50} _{40.00}	Ref	180	-	0	Ref	0	0	180	Refer to record				
	75	Limiting tunnel velocity				63.89	2.00	8.82	19.23	-----	Ref	---	-	0	Ref	0	0	180	No flutter			
	76	216.60	459.8	.3995	69.44	1.81	9.46	19.40	² 22.20	Ref	---	0	0	---	Ref	0	180	Ref	79	324	252	
	77	126.30	345.4	.2996	75.00	1.68	10.20	18.75	18.33	Ref	0	0	0	---	Ref	-	180	Ref	129	0	324	
	78	68.53	251.2	.2174	80.56	1.59	11.11	17.78	17.02	Ref	0	0	0	---	Ref	-	180	Ref	162	---	0	
	79	36.75	183.4	.1581	86.11	1.45	11.76	16.95	16.00	Ref	0	0	0	Ref	180	180	0	Ref	152	158	347	
80	21.11	138.8	.1195	91.67	1.35	11.70	15.91	14.67	Ref	0	0		Ref	180	---	0	Ref	165	---	350		
81	15.28	118.1	.1015	97.22	1.24	11.32	15.10	² 13.33	Ref	0	0	180	Ref	180	0	0	Ref	125	38	346		

²Note oscillograph record, figure 1.



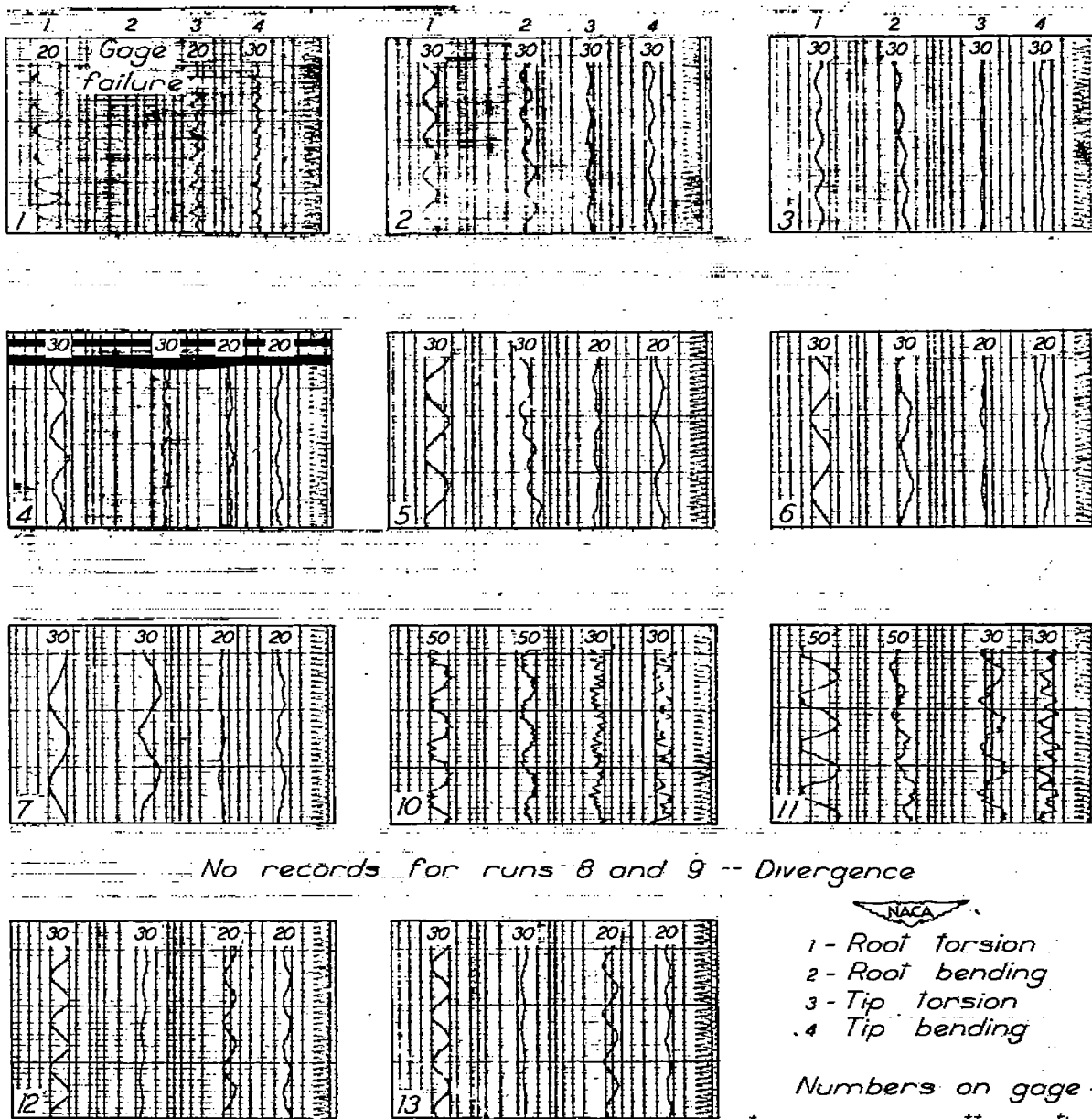
TABLE I.-- EXPERIMENTAL DATA -- Concluded

Model	Run	q_f (lb/sq ft)	V_f (fps)	Mach number	Distance of weight from root (percent l)	Frequencies (cps)				Phase-angle relationship of bending and torsional stresses. (Ref indicates reference strain-gage trace)												
						Natural			Flutter	2nd natural mode				3rd natural mode				Flutter mode				
						1st	2nd	3rd		1	2	3	4	1	2	3	4	1	2	3	4	
		(deg)		(deg)		(deg)				(deg)		(deg)		(deg)		(deg)						
Model O Swept untapered wing; $\Lambda = 60^\circ$ Weight moved along midchord line; $a_w = 0$ Reynolds number $\approx 7514.6V_f$	82	40.92	192.7	0.1670	0	2.94	17.52	22.35	13.33	Ref	180	-	0	Ref	0	0	180	Ref	166	0	9	
	83	39.77	190.0	.1642	13.88	2.96	17.07	22.25	13.64	Ref	180	-	0	Ref	0	0	180	Ref	170	0	28	
	84	36.73	182.7	.1581	25.00	2.93	14.45	22.10	12.00	Ref	180	-	0	Ref	0	0	180	Ref	151	21	8	
	85	41.23	194.3	.1678	30.55	2.90	12.41	21.80	9.82	Ref	180	-	0	Ref	0	0	180	Ref	90	14	34	
	86	41.24	193.9	.1678	36.11	2.89	11.07	21.20	10.00	Ref	180	-	0	Ref	0	0	180	Ref	90	13	27	
	87	57.89	230.3	.1995	41.67	2.73	10.34	20.35	9.52	Ref	180	-	0	Ref	0	0	180	Ref	13	0	340	
	88	74.18	260.4	.2263	47.22	2.60	10.21	19.77	15.63	Ref	180	-	0	Ref	0	0	180	Ref	0	0	---	
	89	73.12	258.3	.2250	52.77	2.42	10.59	19.06	15.58	Ref	180	-	0	Ref	0	0	---	Ref	0	0	0	
	90	77.20	265.1	.2310	58.33	2.24	11.42	18.25	15.28	Ref	180	-	0	Ref	0	0	180	Ref	0	0	---	
	91	95.92	296.1	.2382	63.89	2.08	12.63	17.89	10.00	Ref	180	-	0	Ref	0	0	180	Ref	16	0	---	
	92	86.99	281.4	.2460	69.44	1.90	14.21	17.80	10.00	Ref	180	0	0	Ref	0	0	180	Ref	20	0	---	
	93	75.97	262.8	.2295	75.00	1.73	15.31	18.28	10.91	Ref	180	0	0	Ref	0	0	180	Ref	180	0	---	
	94	71.34	254.2	.2220	80.56	1.60	15.20	18.90	7.89	Ref	180	0	0	Ref	0	0	180	Ref	188	0	---	
	--	No flutter test made				91.67	1.36	14.15	17.35	No record	Ref	180	0	0	Ref	0	0	180	No record			
	95	53.16	218.8	.1908	97.22	1.28	12.54	16.72	5.51	Ref	180	0	0	Ref	0	0	180	Ref	180	0	19	



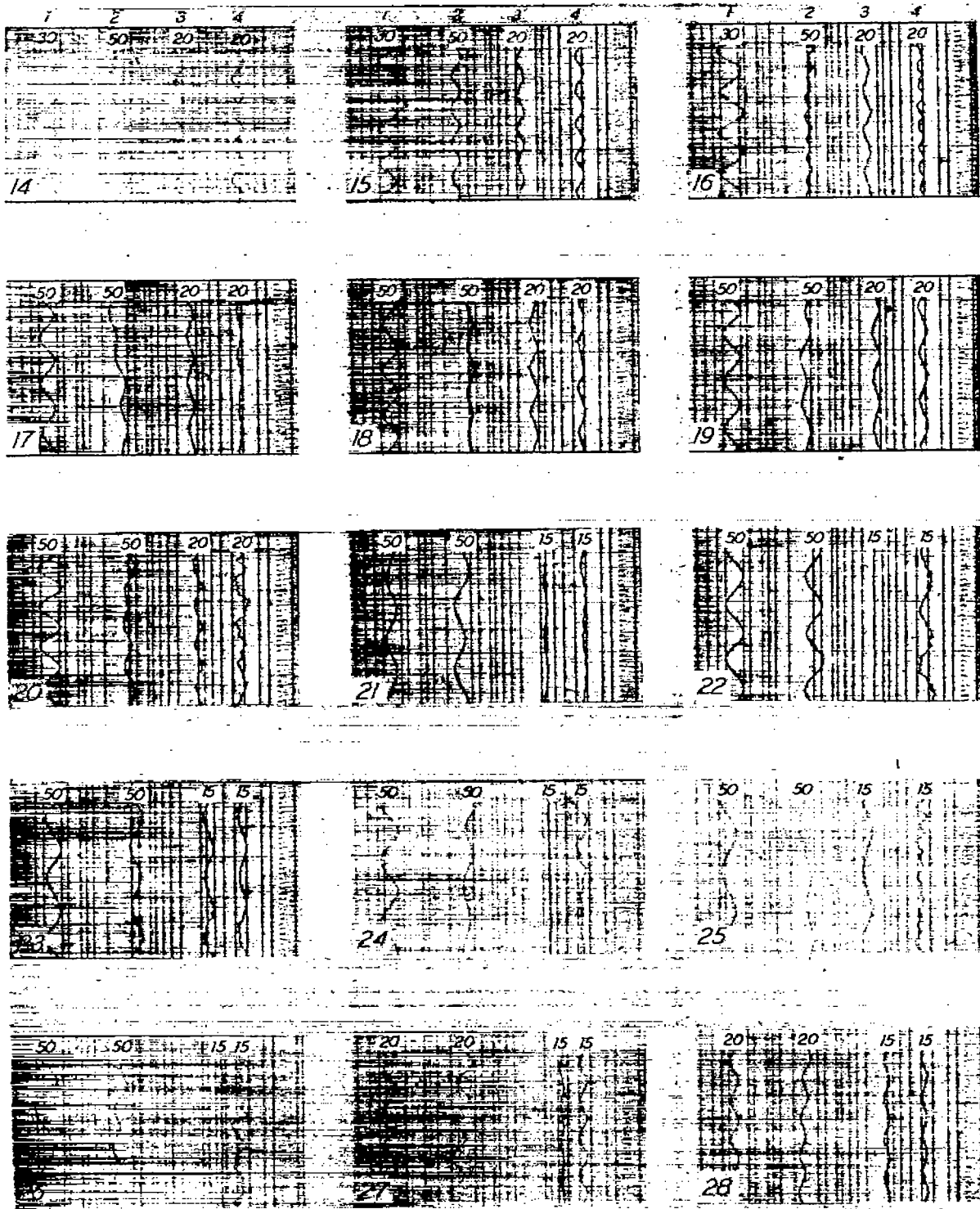
^aNote oscillograph record, figure 1.





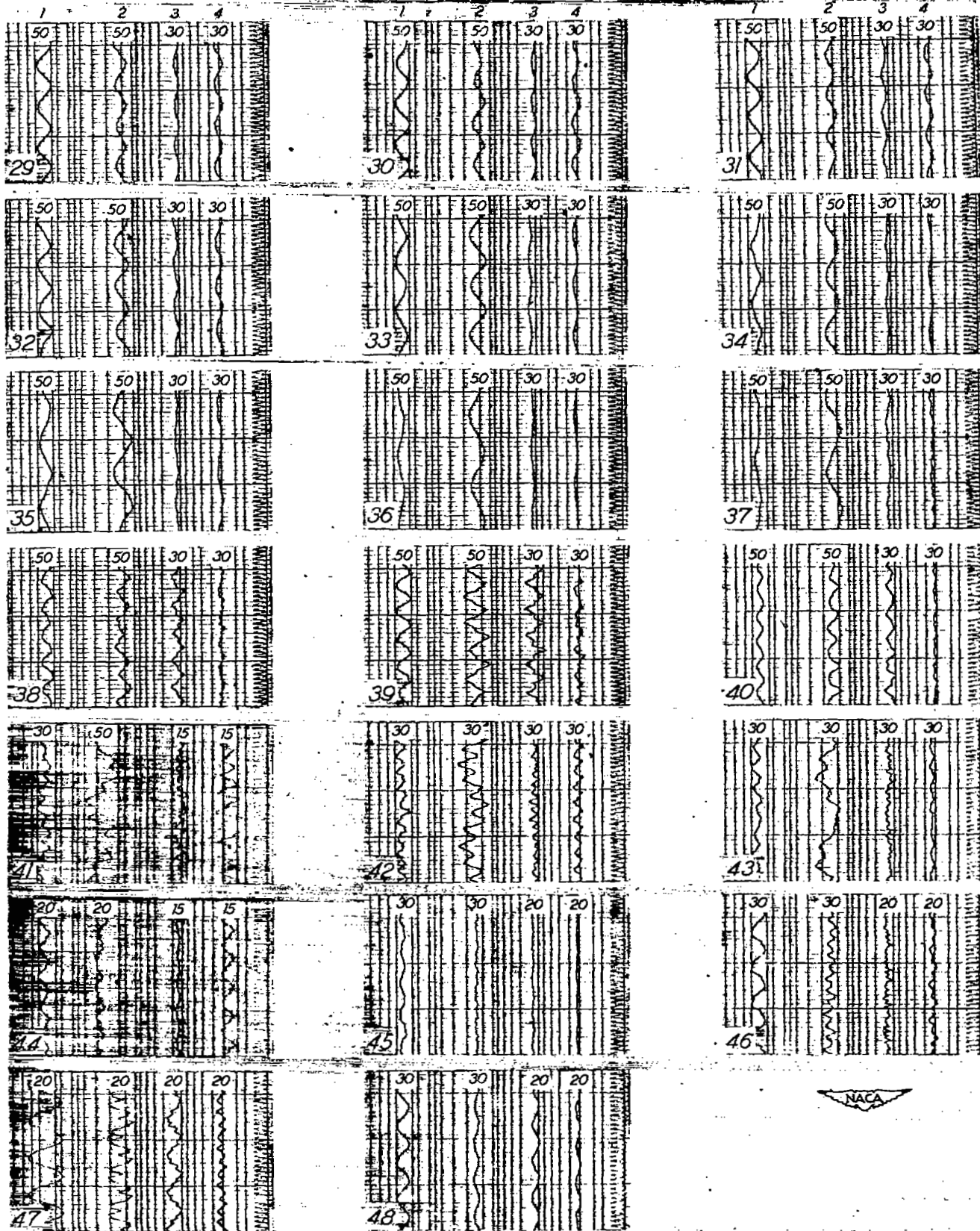
(a) Model A; $\Lambda = 0^{\circ}$; $e_w = -1$.

Figure 1.- Oscillograph records taken at flutter.



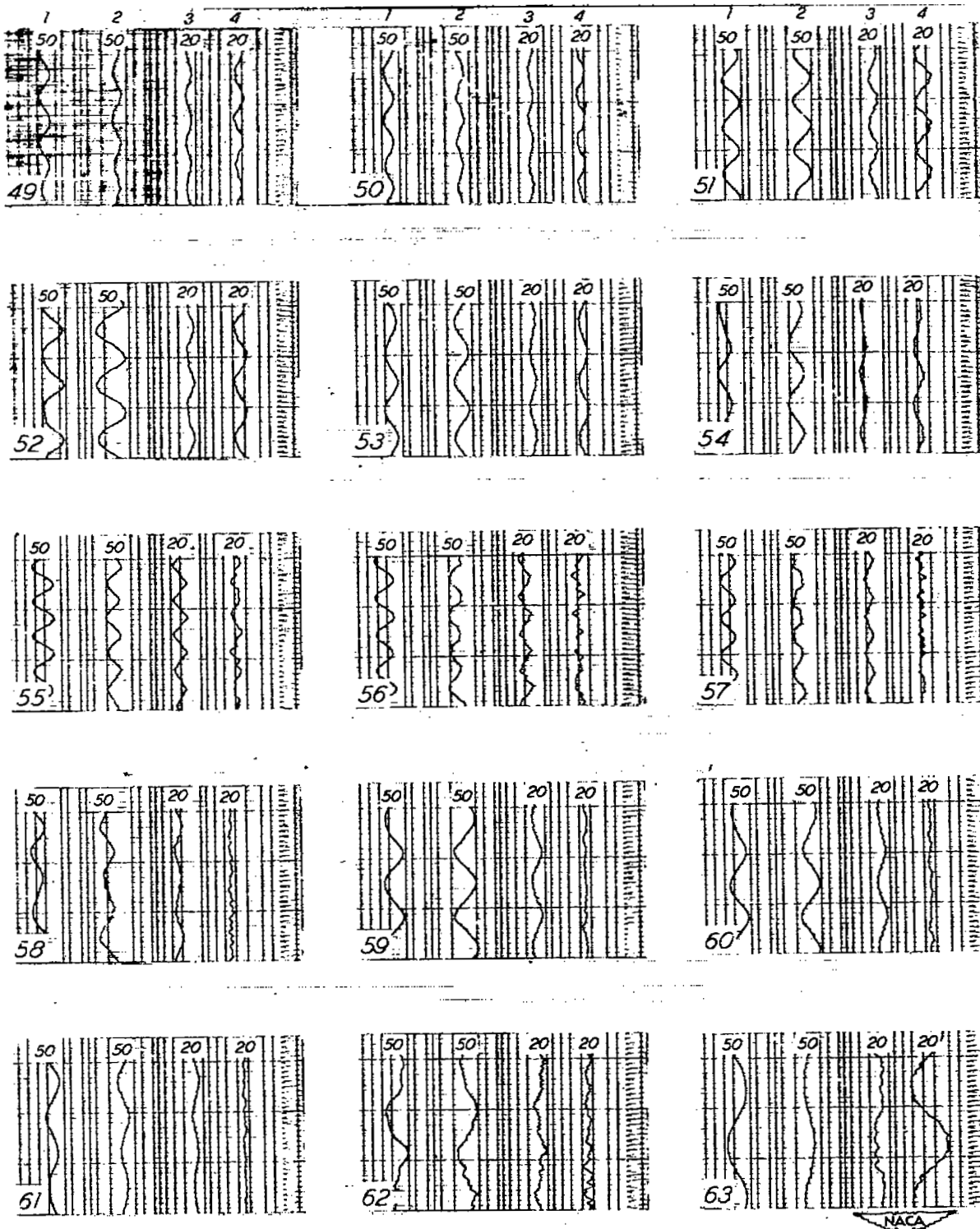
(b) Model A; $\Lambda = 0^\circ$; $e_w = 0$.

Figure 1.- Continued.



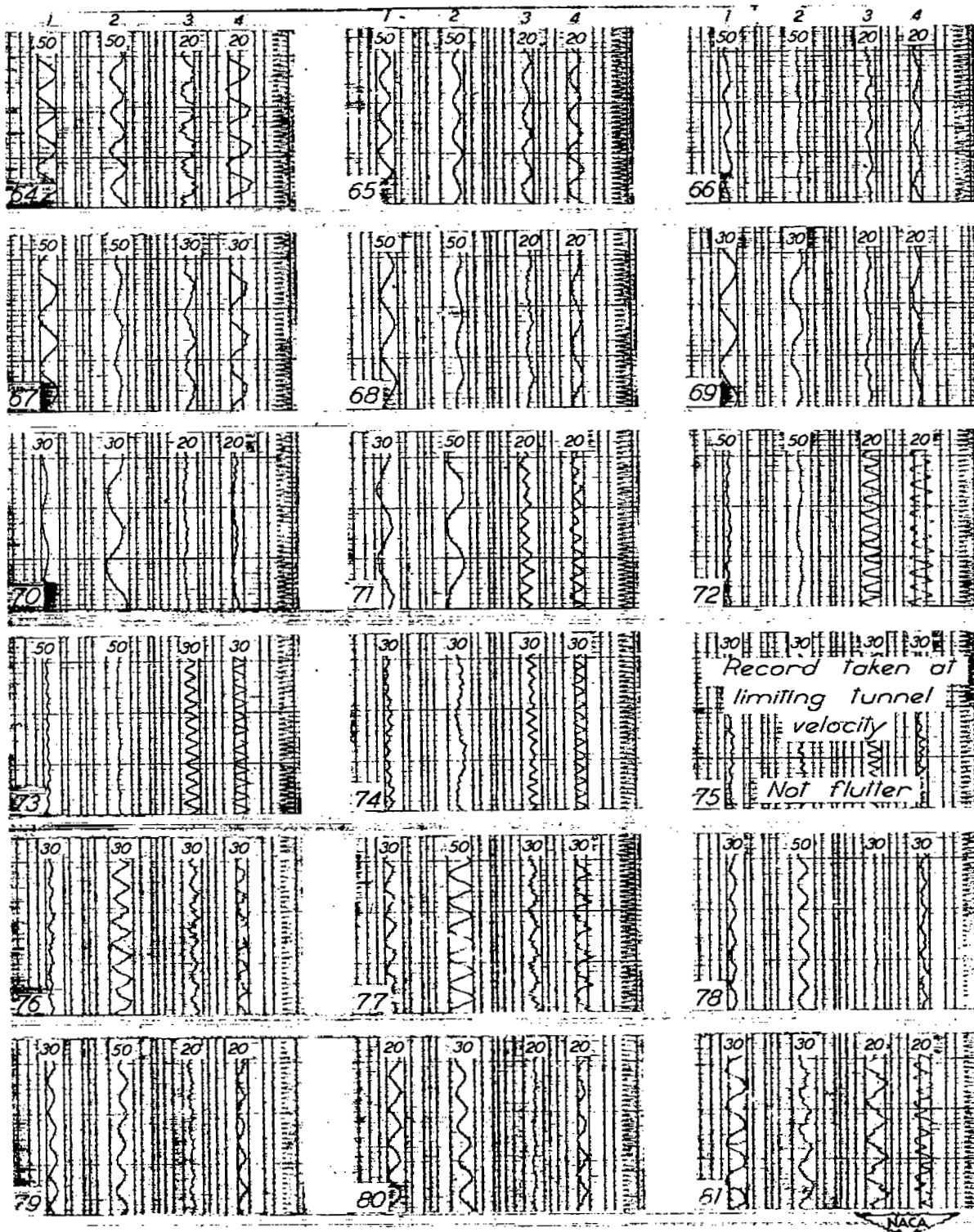
(c) Model B; $\Lambda = 45^\circ$, $e_w = -1$.

Figure 1.- Continued.



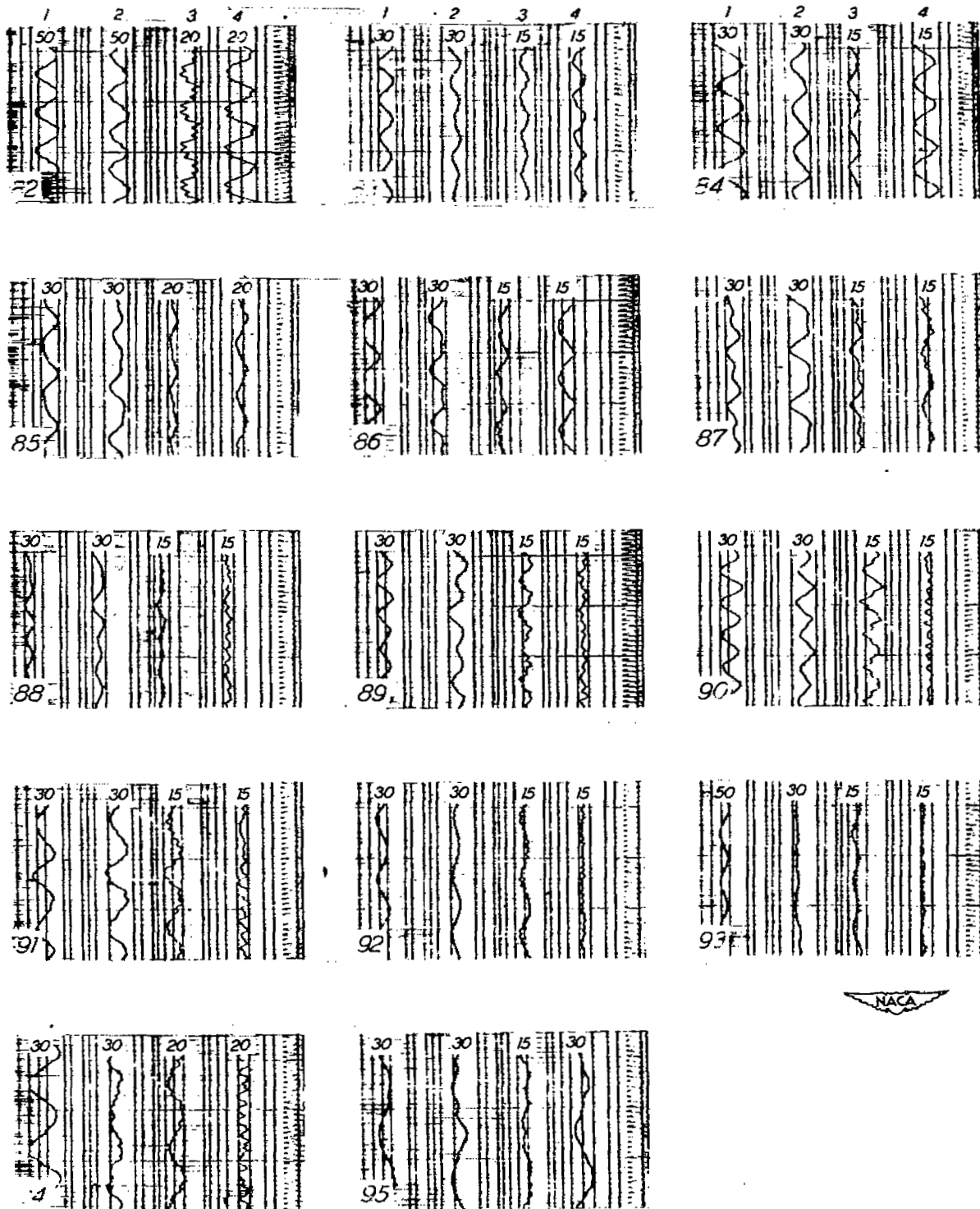
(d) Model B; $\Lambda = 45^\circ$, $e_w = 0$.

Figure 1.- Continued.



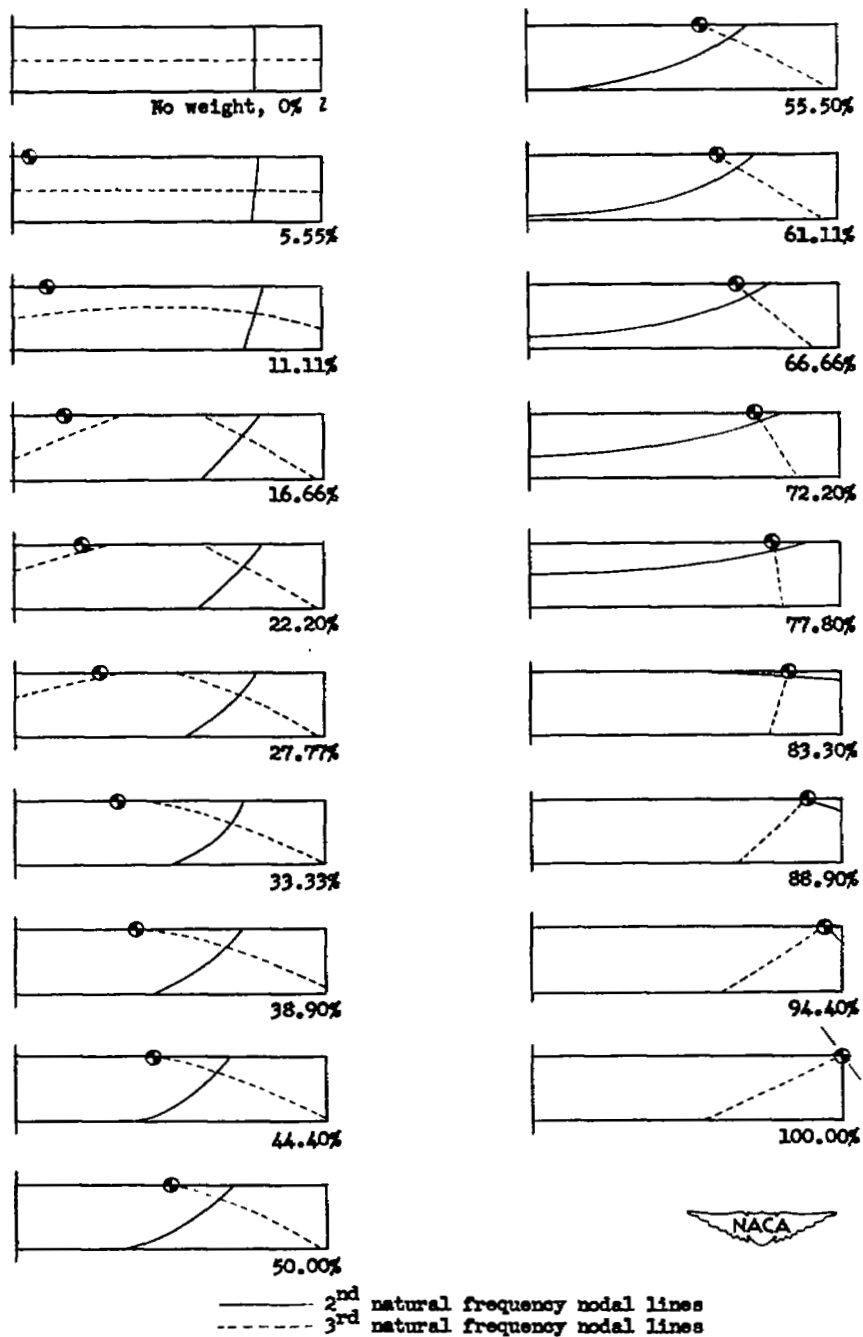
(e) Model C; $\Lambda = 60^\circ$; $e_w = -1$.

Figure 1.- Continued.



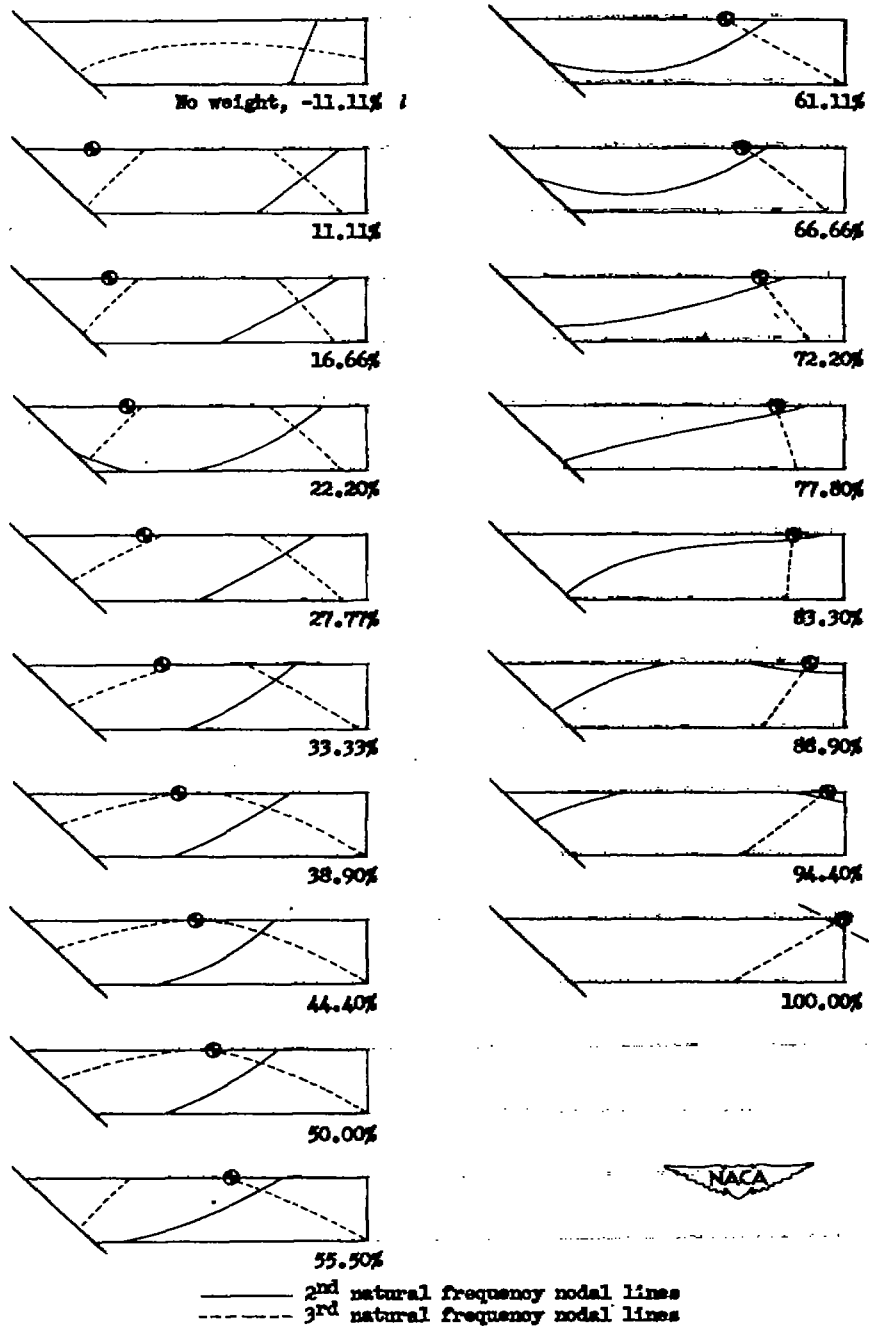
(f) Model C; $\Lambda = 60^\circ$; $e_w = 0$.

Figure 1.- Concluded.



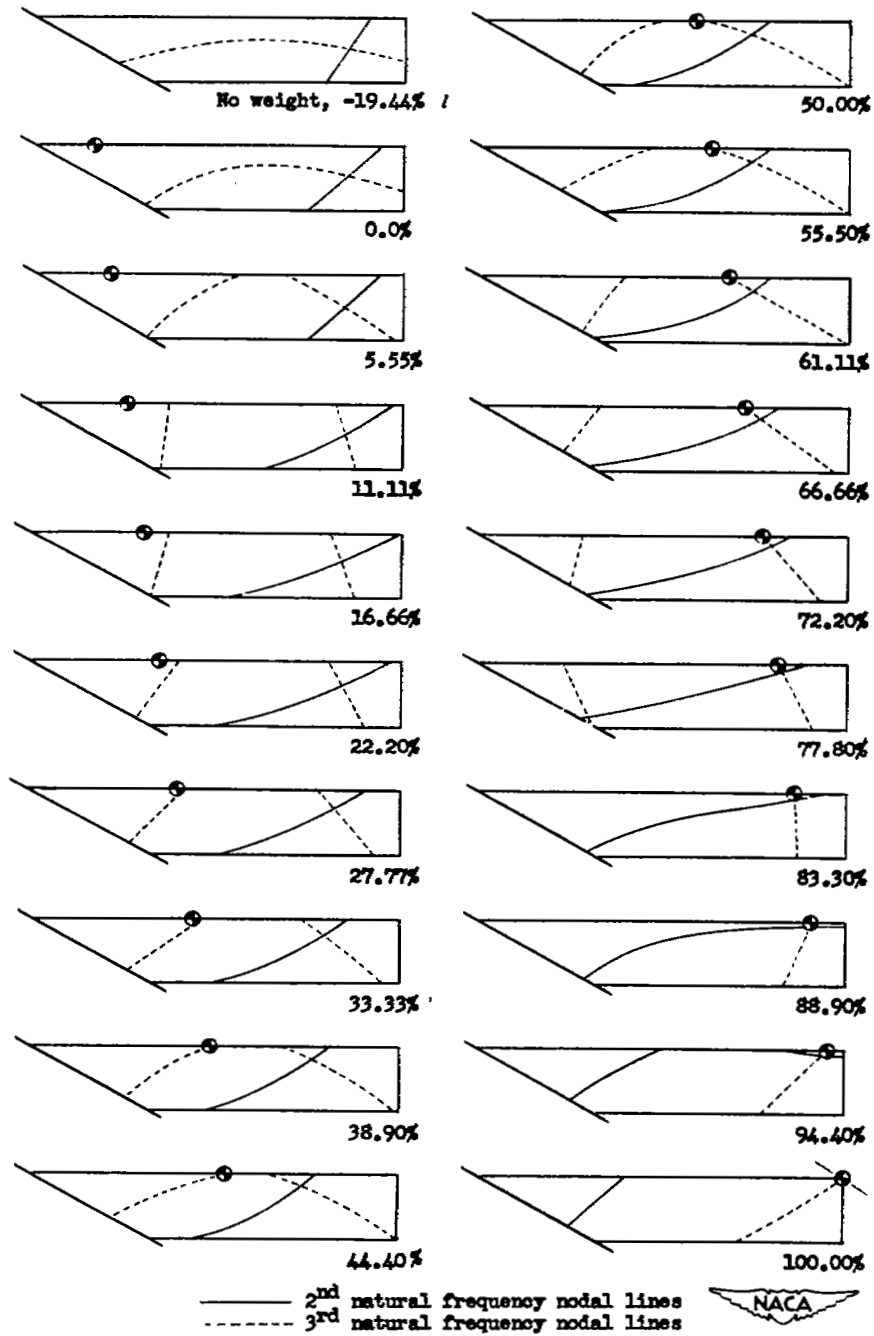
(a) Unswept, untapered wing; $e_w = -1$.

Figure 2.— Progressive change in nodal lines with spanwise weight position.



(b) Swept, untapered wing; $\Lambda = 45^\circ$, $a_w = -1$.

Figure 2.- Continued.



(c) Swept, untapered wing; $\Lambda = 60^\circ$, $e_w = -1$.

Figure 2.— Concluded.

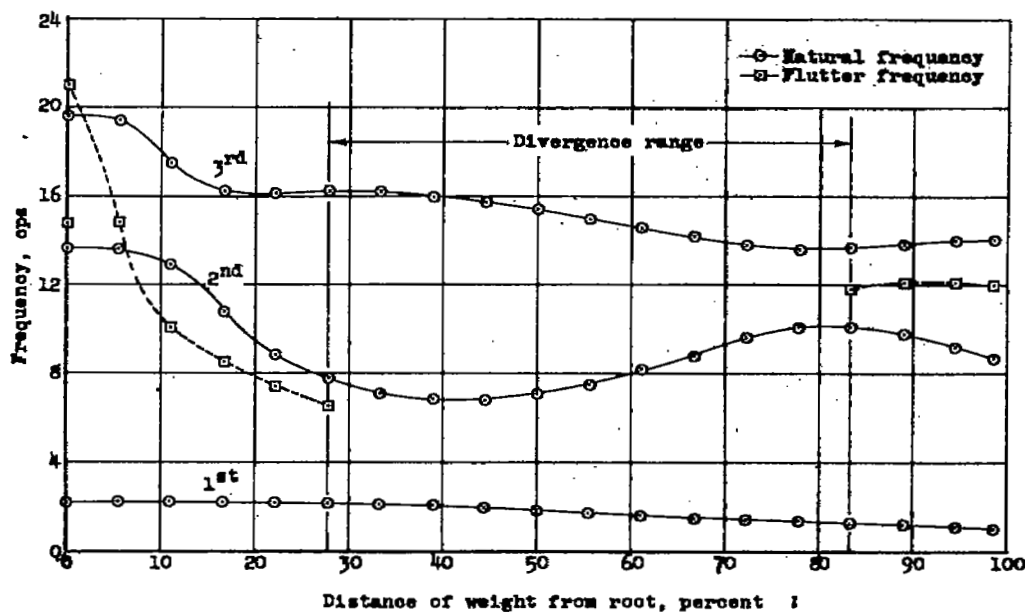
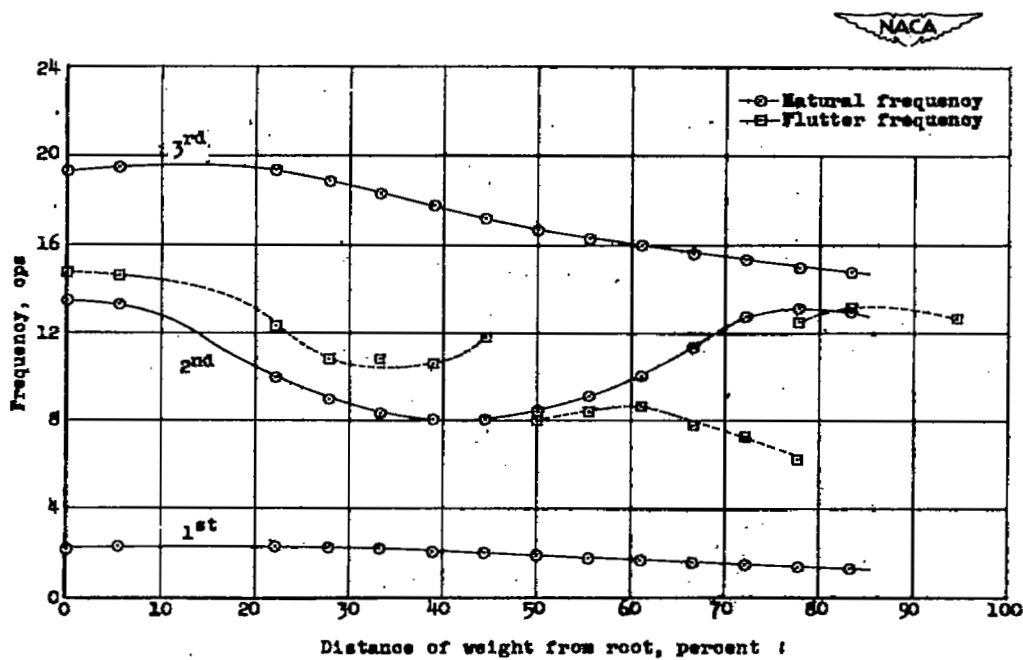
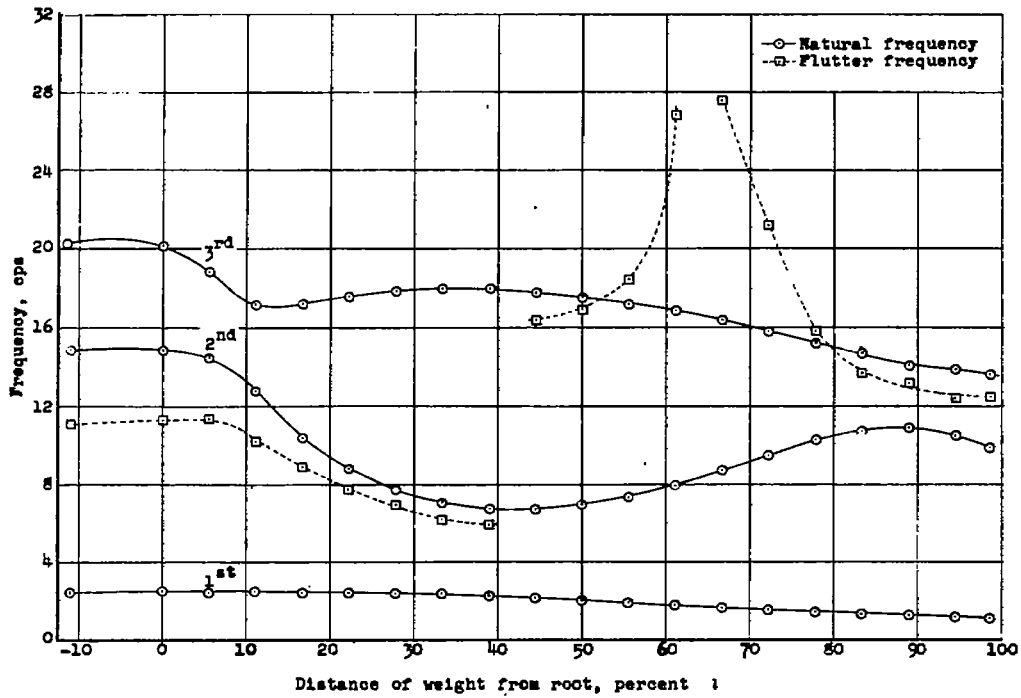
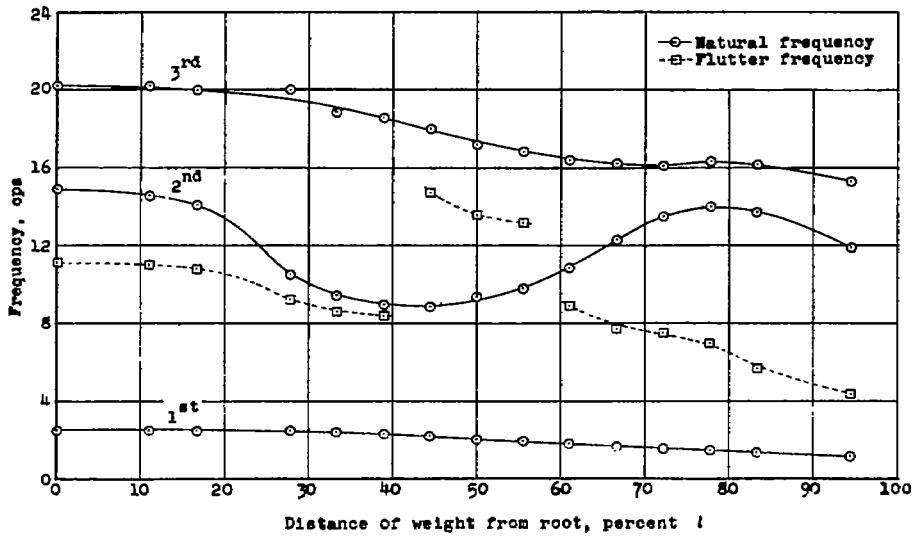
(a) Model A; $\Lambda = 0^\circ$; $e_w = -1$.(b) Model A; $\Lambda = 0^\circ$; $e_w = 0$.

Figure 3.— Variation of first three natural frequencies and flutter frequency with weight position for the various models tested.

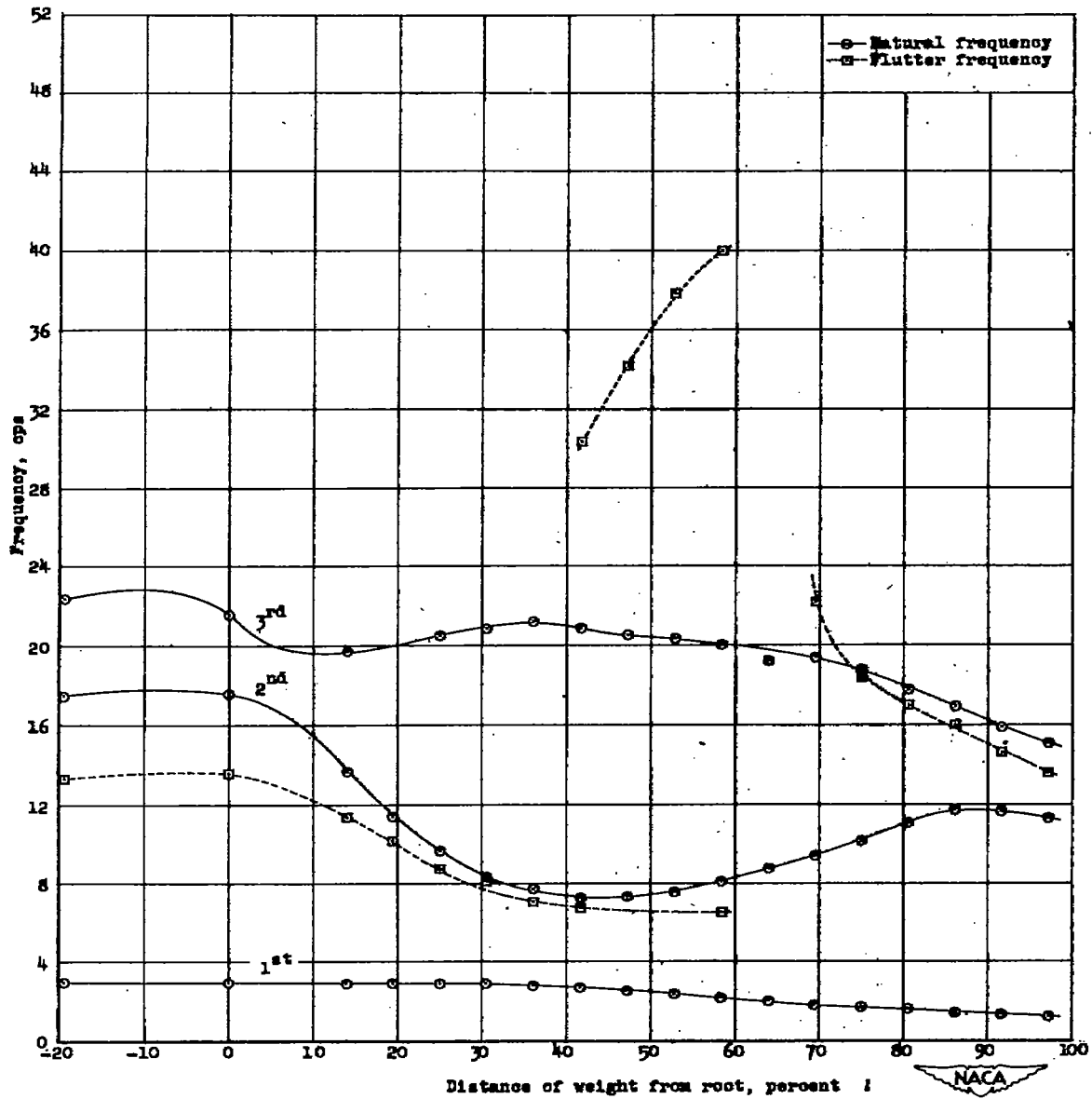


(c) Model B; $\Lambda = 45^\circ$; $e_w = -1$.



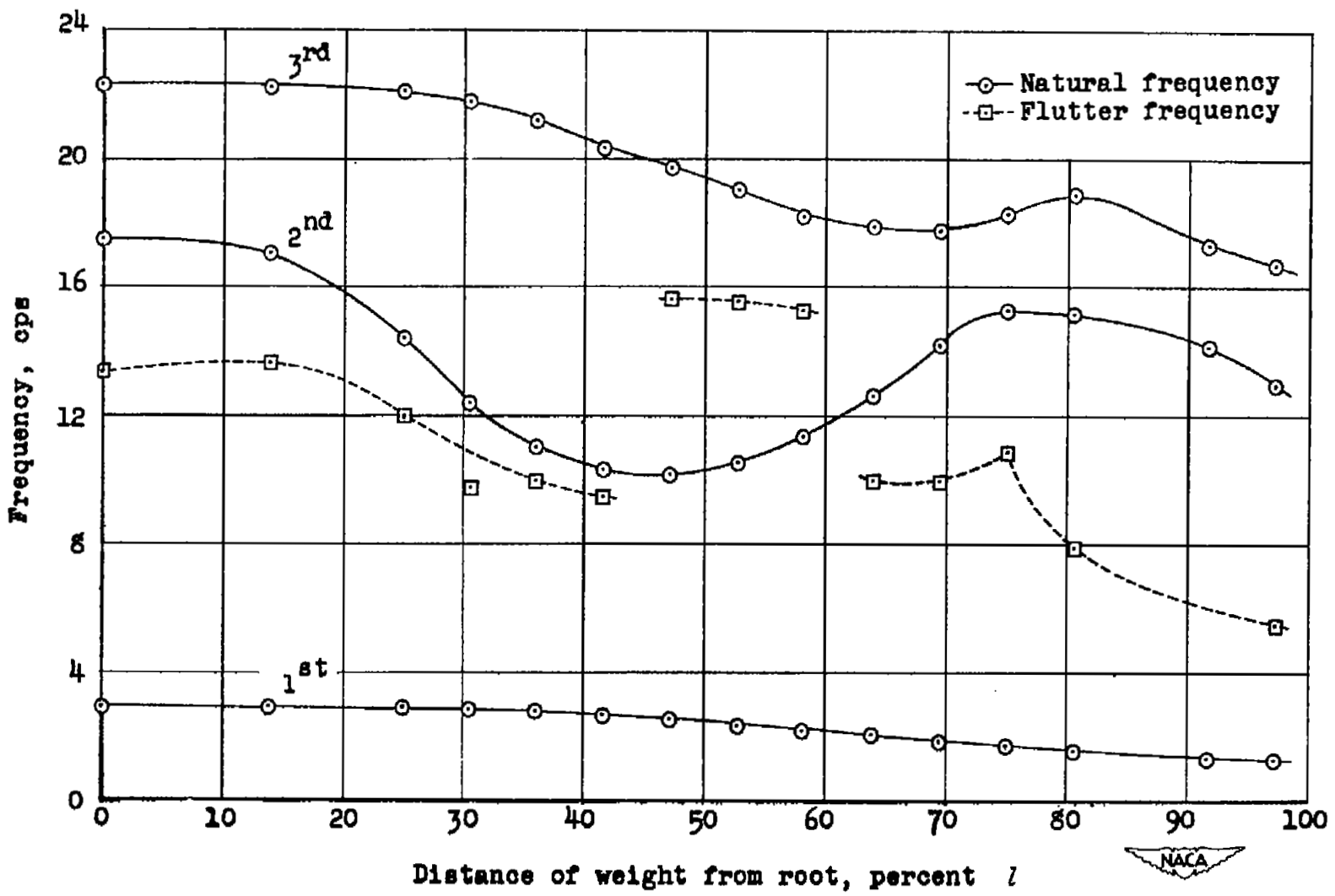
(d) Model B; $\Lambda = 45^\circ$; $e_w = 0$.

Figure 3.- Continued.



(e) Model C; $\Lambda = 60^\circ$; $a_w = -1$.

Figure 3.— Continued.



(f) Model C; $\Lambda = 60^\circ$; $e_w = 0$.

Figure 3.- Concluded.

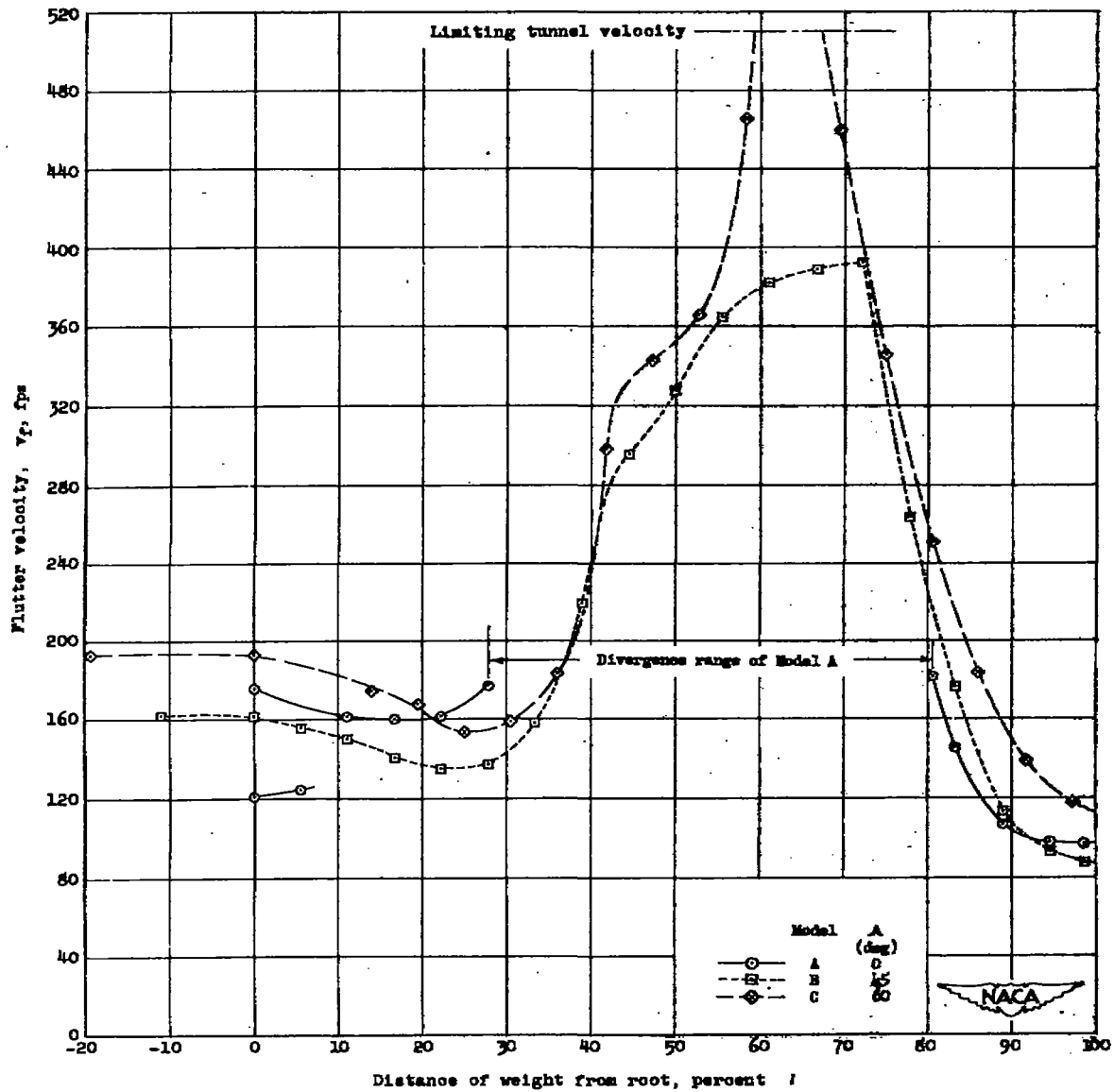
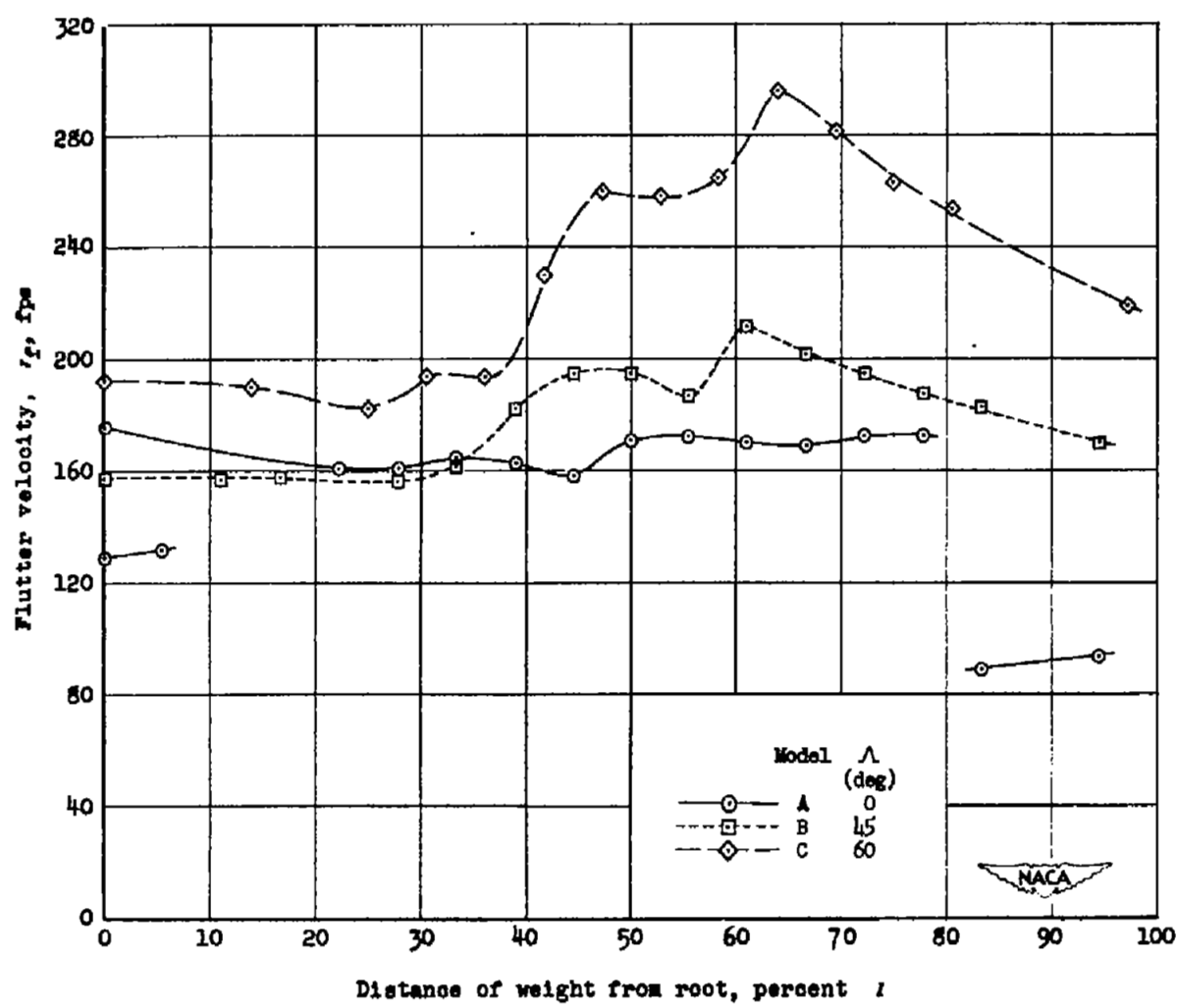
(a) $e_w = -1$.

Figure 4.— Variation of flutter velocity with weight position for the various angles of sweepback.



(b) $e_w = 0$.

Figure 4.- Concluded.

NASA Technical Library



3 1176 01436 7560